ADCONIP 2014 Hiroshima

Temperature Control of EDC Thermal Cracking Furnace with a Coupled ODE and 2D-PDEs Model

Chawin Taweerojkulsri and Chanin Panjapornpon

Abstract— This paper presents a new control technique for the EDC thermal cracking furnace modeled by sets of ordinary differential equation (ODE) and 2D-partial differential equations (PDEs). The dynamics of coupled 2D-PDEs-ODE model have been divided into 2 subsystems, set of state variables of the internal and external cracking coil. With the concept of input-output (I/O) linearization, these inner and outer dynamics are applied to design the setpoint tracking calculator and the approximate I/O feedback controller respectively. The first-order error dynamics and the finite-based, open-loop observer are integrated with the proposed controller system to compensate the model mismatch and to predict the unmeasured state information. The performances of the proposed method are evaluated through the servo test. The results showed that the control method effectively forces the output to the desired setpoint.

I. Introduction

Vinyl chloride monomer (VCM) is a raw material for Poly Vinyl Chloride (PVC) production. It is typically obtained from the cracking of 1,2-dichloroethane (EDC) under 400-500°C, of which hydrogen chloride (HCl) is a byproduct. The reaction can proceed by following:

$$\underset{EDC}{C_2H_4Cl_2(g)} \rightarrow \underset{VCM}{C_2H_3Cl(g)} + \underset{Hydrogen\ Chloride}{HCl(g)} \quad (1)$$

The EDC cracking rate strongly depends on the reaction temperature; increase on the reaction temperature results in the high cracking rate. The EDC vapor is reacted along the lengthy empty coil suspended in the chamber of the gas-fired cracking furnace. Furnace dynamics are highly nonlinear due to the spatial distributed temperature and concentration of the gas inside the cracking coil, as well as the effect of the temperature of the furnace wall. These complex behaviors lead to deteriorate the performance of the gas temperature control by a proportional integral derivative (PID) controller. They may cause off spec of the products, thermal runaway, plant shut down or, in the worst case, explosion. Therefore, the control method that can handle the temperature of the cracking furnace effectively is needed to achieve a high quality product.

Research works regarding the temperature control of the furnace were mostly focused on the dynamics of the tubular reactor. Some works applied the model reduction technique to lump the reactor model before performing the controller synthesis. For example, the PDE was lumped by Galerkin method and then applied with infinite dimensional state feedback [1] lumped by method of characteristic and applied with robust control [2] and lumped by infinite dimensional method and applied with the linear quadratic regulator (LQR) [3]. Some works use the process data to develop an empirical model by the neural network method before applied with the robust control [4] or generic model control (GMC) [5]. Besides, there are few works considering to the interaction of wall radiation in the control of furnace. Masoumi and colleagues [6] studied the temperature control of the naphtha thermal cracking with multi cracking coils by using the PI controller. The desired setpoints were obtained from the optimization of the temperature profile. In Zeybek [7], the outlet gas temperature is controlled by manipulating the fuel mass flow rate by using the adaptive heuristic controller based on three layers of feed forward artificial network (ANN). Panjapornpon et al. [8] proposed the control of coupled PDE-ODEs for EDC cracking furnace by using approximate I/O linearization; the tube temperature was controlled by manipulating the fuel gas flow while the mass production rate of VCM was handled by the PI controller by manipulating the EDC feed. The furnace model was developed by assuming a plug-flow velocity profile and neglecting the effect of the radius heat transfer. However, there are some works mentioned about significant difference of predicted process dynamics when the redial effect and velocity profile has been taken into accounted [9-10]. This brings about the question of the improvement of control performance when the 2D model has been applied. In fact, the gas temperature represented the reaction temperature is measured by a thermocouple installed at the center of the exit tube. The EDC conversion calculated by the 1D model will be lower than the actual process value. The performance of 1D-based PDE-ODE controller in practice may deteriorate due to a significant process-model mismatch.

This work presents a new structure of the coupling 2D PDEs-ODE model for the EDC cracking furnace by using the I/O linearization. The dynamics of EDC cracking furnace consist of the EDC concentration and gas temperature considered as the internal states and the tube temperature and furnace wall considered as external states. All the dynamics are described by PDEs except the furnace wall dynamics described by ODE. The purpose of this work is to control the gas temperature at the exit tube by manipulating the fuel gas flow. Instead of applying the I/O controller to the objective directly, the internal subsystem is

Chanin Panjapornpon (corresponding author: 662-797-0999 ext. 1230; e-mail: fengcnp@ku.ac.th) and Chawin Taweerojkulsri are with Center of Excellence on Petrochemical and Materials Technology, Department of Chemical Engineering, Faculty of Engineering, Kasetsart University, Bangkok 10900, Thailand.

used for developing the setpoint tracking calculator while the external is applied for the controller synthesis. The gas temperature is applied with I/O linearization to develop the mapping function of the equivalent tube temperature setpoint for the I/O feedback controller. The first-order error dynamics and the finite-based, open-loop observer are integrated into the control system to eliminate the offset and predict the unmeasured state information. An advantage of proposed control method with the partitioning state dynamics is to reduce the complexity of the controller equation with a better predicting quality by using the 2D process model.

II. Mathematic Model of EDC Cracking Furnace

A simple process scheme of an EDC cracking furnace is shown in Fig.1. In the operation, EDC vapor is fed to the cracking coil and converted to be VCM and HCl. The natural gas is used as a combustion fuel to supply the energy to the furnace to rise up the furnace wall temperature (T_w). The furnace wall radiates and transfers the energy to the tube inside leading to the change of the tube temperature (T_t), the gas temperature (T_g) and EDC concentration (C_{EDC}) consequently.

In this work, the proposed control strategy is applied with 2D PDEs-ODE model of EDC cracking furnace. The following model assumptions are applied:

1) All gases in the system are ideal.
2) Only the reaction in (1) occurring in the tube is concerned.
3) Neglect effects of all elbows and fittings; straight tube is assumed.
4) The properties of gases in the tube are constant.
5) The tube temperature is varied along the z-direction only because of the pipe thickness << the coil distance.
6) The gas temperature and EDC concentration are varied in both the radius and distance of the coil.

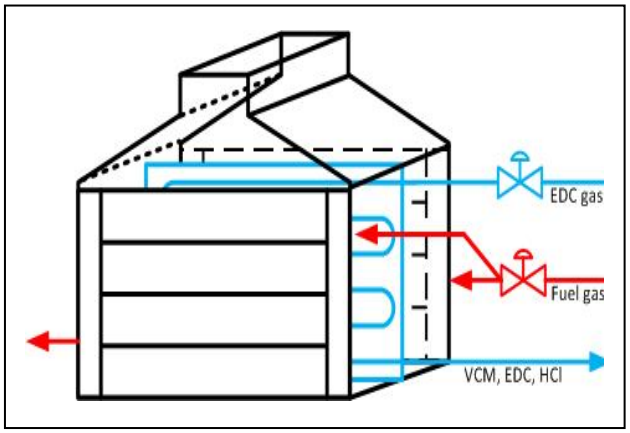

Fig. 1. Continuous stirred tank reactor with cooling system

The dynamic models of the cracking furnace are represented by following equations

- The dynamics of EDC concentration and reactor temperature in the cracking coil:

$$\frac{\partial C_{EDC}}{\partial t} = -v\frac{\partial C_{EDC}}{\partial z} + \frac{k_g}{\rho_g C_{pg}}\frac{1}{r}\frac{\partial}{\partial r}\left(r\frac{\partial C_{EDC}}{\partial r}\right) + r_{EDC}$$

$$\frac{\partial T_g}{\partial t} = -v\frac{\partial T_g}{\partial z} + \frac{k_g}{\rho_g C_{pg}}\frac{1}{r}\frac{\partial}{\partial r}\left(r\frac{\partial T_g}{\partial r}\right) + \frac{A_i F\sigma}{V_t \rho_g C_{pg}}(T_t^4 - T_g^4) + \frac{|r'''_{EDC}|(\Delta H)_{EDC}}{\rho_g C_{p_g}}$$

$$r_{EDC} = -k_0 e^{-\frac{E_a}{RT_g}} C_{EDC} \tag{2}$$

with the following boundaries and initial conditions:

for the EDC concentration,

$$BC1: \quad \frac{\partial C_{EDC}}{\partial r}(0,z,t) = 0$$

$$BC2: \quad \frac{\partial C_{EDC}}{\partial r}(R_i,z,t) = 0$$

$$BC3: \quad C_{EDC}(r,0,t) = C_{EDC,0}$$

$$IC1: \quad C_{EDC}(r,z,0) = C_{EDC,0}$$

and for the gas temperature,

$$BC4: \quad \frac{\partial T_g}{\partial r}(0,z,t) = 0$$

$$BC5: \quad T_g(R_i,z,t) = T_t(z,t)$$

$$BC6: \quad T_g(r,0,t) = T_{g,0}$$

$$IC2: \quad T_g(r,z,t=0) = T_{g,0}$$

The velocity profile of the gas flowing in the coil is referred to an empirical/analytical solution of $k-\varepsilon$ turbulence model in [11]:

$$v(r) = 12.85\sqrt{\frac{-dP/dz \cdot R_i}{2\cdot\rho_g}} + \sqrt{\frac{-dP/dz \cdot R_i}{0.32\cdot\rho_g}} \cdot \ln\left(\frac{R_i - r}{26\cdot\frac{\mu}{\rho_g}\cdot\sqrt{\frac{2\cdot\rho_g}{-dP/dz\cdot R_i}}}\right) \tag{3}$$

where the total pressure gradient and fanning friction factor are approximated by using analytical/empirical equations proved from the Moody friction [12]:

$$-\frac{dP}{dz} \approx \frac{\Delta P}{L}$$

$$\Delta P = -\frac{f\cdot\rho_g\cdot v_{av}^2 L}{4\cdot R_i} \tag{4}$$

$$f = \frac{0.184}{\mathrm{Re}^{0.2}}, \ \mathrm{Re} \geq 20{,}000$$

The average velocity is calculated by

$$v_{av} = \frac{2}{R_i^2}\int_0^{R_i} r v_z(r)dr \tag{5}$$

- The dynamics of tube and furnace wall temperature:

$$\frac{dT_t}{dt} = \frac{1}{\rho_t c_{p,t}} k_t \frac{\partial^2 T_t}{\partial z^2} + \frac{1}{\rho_t c_{p,t} V_{th,t}}\Big[A_w F\sigma(T_w^4 - T_t^4) - A_i F\sigma(T_t^4 - T_g^4) - \frac{2\pi L}{\frac{\ln(R_o/R_i)}{k_t} + \frac{1}{R_o h_f}}(T_w - T_t)\Big] \tag{6}$$

$$\frac{dT_w}{dt} = \frac{\dot{m}_{fuel}\Delta H_{comb} - \sigma F A_w (T_w^4 - T_t^4)}{(m_w c_{p_w})}$$

with the boundary and initial conditions:

$$BC7: \quad T_t(0,t) = T_{t,0}$$

$$BC8: \quad \frac{\partial T_t}{\partial z}(L,t) = 0$$

$$IC3: \quad T_t(z,0) = T_{t,0}$$

$$IC4: \quad T_w(z,0) = T_{w,0}$$

All process parameters defined in the notation section are given in Table I.

The model of the fired-furnace in (2)-(6) described by partial differential equations in r and z coordinates and ordinary differential equation can be grouped into two subsystem.

The subsystem of (7.a) expresses the interaction of the state variables inside the cracking coil and the subsystem in (7.b) expresses the interaction of the state variables outside the cracking coil and the radiating wall.

$$\frac{\partial x_{p1}(r,z,t)}{\partial t} = -a\frac{\partial x_{p1}}{\partial z} + b\frac{1}{r}\frac{\partial}{\partial r}\left(r\cdot\frac{\partial x_{p1}}{\partial r}\right) + M(x_{p1}, x_{p2}) \tag{7.a}$$

$$\begin{aligned} \frac{\partial x_{p2}(z,t)}{\partial t} &= c\frac{\partial^2 x_{p2}}{\partial z^2} + N(x_{p1}, x_o(t)) + O(x_{p2}, x_o) \\ \frac{dx_o(t)}{dt} &= f(x_o, x_{p2}, u(t)) \\ y &= h(x_{p1}) \end{aligned} \tag{7.b}$$

with the initial and boundary conditions of (7.a):

$$B.C. \begin{cases} \dfrac{\partial x_{p1}(0,z,t)}{\partial r} = 0, \\ x_{p1}(R,z,t) = x_{p2}(z,t) \text{ or } \dfrac{\partial x_{p1}(R,z,t)}{\partial r} = 0, \\ x_{p1}(r,0,t) = x_{p1}(r,t) \end{cases}$$

$$I.C. \quad x_{p1}(r,z,0) = x_{p1,0}(r,z)$$

and the initial and boundary conditions of (7.b):

$$B.C. \begin{cases} x_{p2}(0,t) = x_{p2}(t), \\ \left.\dfrac{\partial x_{p2}}{\partial z}\right|_{z=L} = 0 \end{cases}$$

$$I.C. \begin{cases} x_{p2}(z,0) = x_{p2,0}(z), \\ x_o(t=0) = x_{o,0} \end{cases}$$

where $x_{p1}(r,z,t)$ denotes the vector of the state variables depending on r and z coordinates, $x_{p2}(z,t)$ denotes the state variable of the external tube dynamics which is directly

Table I.
PARAMETER VALUES FOR THE EDC CRACKING FURNACE

Symbol	Quantity	Value
A_w	Area of the furnace wall	218 m^2
C_{pg}	Average heat capacity of cracked gases	8.5059 m^3
C_{pt}	Heat capacity of the tube	444 J/kg K
C_{pw}	Heat capacity of the furnace wall	1000 L/kg K
D_i	Internal tube diameter	0.19 m
E_a	Activation energy	1.15×10^5 J/mol
F	Shape factor	1
ΔH_{EDC}	Heat of reaction	-7.1×10^4 J/mol
ΔH_{comb}	Heat of combustion	4.25×10^7 J/mol
k_0	Kinetic constant	1.15×10^7
k_g	Thermal conductivity of gases in tube	2.655×10^{-2} W/m K
k_t	Thermal conductivity of the tube	20.5 W/m K
L	Tube length	300 m
m_t	Tube weight	7.783×10^3 kg
m_w	Mass of furnace wall	4.191×10^5 kg
$\dot{m}_f$	Mass flow rate of the fuel	0-0.6 kg/s
Mw_{EDC}	EDC molecular weight	98.96 g/mol
Pe	Thermal Peclet number	8.57×10^5 –2.00×10^6
Pr	Prandl number	0.72
R	Gas constant	8.314 J/mol K
R_i	Internal tube radius	0.095 m
R_o	External tube radius	0.1 m
Re	Reynolds number	1.19×10^6 –2.78×10^6
V_t	Pipe volume	8.5059 m^3
ρ_g	Cracked gas density	35.43 kg/m^3
ρ_t	Tube density	8470 kg/m^3
σ	Stefan-Boltzman constant	5.67×10^{-8} W/m^2 K
μ	Viscosity of cracked gases	1.695×10^{-5} kg/m s
v	Feed velocity	5 m/s

affected by x_o, $x_o(t)$ denotes the state variable which depend on time, y denote the output variable, $z \in [0, L]$ and $r \in [0, R_o]$ are spatial coordinates, $t \in [0, \infty]$ is the time, and $u(t)$ is the manipulated variable.

III. CONTROL SYSTEM DESIGN

In our case, the process model is highly complex due to coupled PDEs and ODE. The control objective is to regulate the output at the exit of the tube (y=L), the state in the subsystem (7.a), by adjusting the input (u) in the subsystem (7.b). To reduce complexity of the controller design, in this work, the set of PDE in (7.a) described the internal tube dynamics will be used to create a tracking correlation between the output (y) and the distributed state variable related to the lumped dynamics (x_{p2}). The set of coupling PDEs-ODE in (7.b) described the external tube dynamics will be used to develop the I/O feedback controller that the control action (u) is obtained by solving closed-loop response of x_{p2}. A schematic diagram of the control system shown in Fig. 2 is proposed. The control system consists of a setpoint tracking calculator, I/O linearizing controller, and a finite-based, open-loop observer. More details of the control system design are given as follows.

A. Setpoint tracking calculator

The input/output linearization is a method that creates a linear relationship between input and output based on the coordinate transformation. It is traditionally applied for the ODE system. For the application of PDEs-ODEs system, let consider the system in (8).

$$\begin{aligned} \frac{d\bar{x}}{dt} &= f(\bar{x}, \bar{x}_r, \bar{x}_{rr}, \bar{x}_z, \bar{x}_{zz}, \bar{u}) \\ \bar{y}_L &= h(\bar{x})\big|_{r=0,z=L} \end{aligned} \tag{8}$$

where $\bar{x}$ is the vector of state variables, $\bar{x}_z = \partial\bar{x}/\partial z$ and $\bar{x}_r = \partial\bar{x}/\partial r$ are the first-order spatial derivatives of $\bar{x}$ respect to z-direction and r-directions, $\bar{x}_{zz} = \partial^2\bar{x}/\partial z^2$ and $\bar{x}_{rr} = \partial^2\bar{x}/\partial r^2$ are the second-order spatial derivatives of $\bar{x}$ respect to z-direction and r-direction, $\bar{u}$ is the manipulated input and h is the vector of nonlinear functions. The relative order of the controlled output y_L, r, can be defined by following notation:

$$\begin{aligned} y_L &= h(\bar{x})\big|_{r=0,z=L} \\ \frac{dy_L}{dt} &\triangleq \left[\frac{h}{\partial\bar{x}}\frac{\partial\bar{x}}{\partial t}\right]_{z=L} = h^1\left(\bar{x}, \bar{x}_r, \bar{x}_{rr}, \bar{x}_z, \bar{x}_{zz}\right)\big|_{r=0,z=L} \\ &\vdots \\ \frac{d^{r-1}y_L}{dt^{r-1}} &\triangleq \left[\begin{array}{l} \frac{\partial h^{r-2}}{\partial\bar{x}}\frac{\partial\bar{x}}{\partial t} + \frac{\partial h^{r-2}}{\partial\bar{x}_r}\frac{\partial\bar{x}_r}{\partial t} + \frac{\partial h^{r-2}}{\partial\bar{x}_{rr}}\frac{\partial\bar{x}_{rr}}{\partial t} \\ + \frac{\partial h^{r-2}}{\partial\bar{x}_z}\frac{\partial\bar{x}_z}{\partial t} + \frac{\partial h^{r-2}}{\partial\bar{x}_{zz}}\frac{\partial\bar{x}_{zz}}{\partial t} + \ldots + \frac{\partial^{r-2}}{\partial t^{r-2}}(\bar{x}_{zz}) \end{array}\right]_{r=0,z=L} \\ &= h^{r-1}\left(\begin{array}{l} \bar{x}, \bar{x}_r, \bar{x}_{rr}, \bar{x}_z, \bar{x}_{zz}, \frac{\partial\bar{x}_r}{\partial t}, \ldots, \frac{\partial^{r-2}}{\partial t^{r-2}}(\bar{x}_r), \frac{\partial\bar{x}_{rr}}{\partial t}, \ldots, \\ \frac{\partial^{r-2}}{\partial t^{r-2}}(\bar{x}_{rr}), \frac{\partial\bar{x}_z}{\partial t}, \ldots, \frac{\partial^{r-2}}{\partial t^{r-2}}(\bar{x}_z), \frac{\partial\bar{x}_{zz}}{\partial t}, \ldots, \frac{\partial^{r-2}}{\partial t^{r-2}}(\bar{x}_{zz}) \end{array}\right)\Bigg|_{r=0,z=L} \\ \frac{d^r y_L}{dt^r} &\triangleq \left[\begin{array}{l} \frac{\partial h^{r-1}}{\partial\bar{x}}\frac{\partial\bar{x}}{\partial t} + \frac{\partial h^{r-1}}{\partial\bar{x}_r}\frac{\partial\bar{x}_r}{\partial t} + \frac{\partial h^{r-1}}{\partial\bar{x}_{rr}}\frac{\partial\bar{x}_{rr}}{\partial t} \\ + \frac{\partial h^{r-1}}{\partial\bar{x}_z}\frac{\partial\bar{x}_z}{\partial t} + \frac{\partial h^{r-1}}{\partial\bar{x}_{zz}}\frac{\partial\bar{x}_{zz}}{\partial t} + \ldots + \frac{\partial^{r-1}}{\partial t^{r-1}}(\bar{x}_{zz}) \end{array}\right]_{r=0,z=L} \\ &= h^r\left(\begin{array}{l} \bar{x}, \bar{x}_r, \bar{x}_{rr}, \bar{x}_z, \bar{x}_{zz}, \frac{\partial\bar{x}_r}{\partial t}, \ldots, \frac{\partial^{r-1}}{\partial t^{r-1}}(\bar{x}_r), \frac{\partial\bar{x}_{rr}}{\partial t}, \ldots, \\ \frac{\partial^{r-1}}{\partial t^{r-1}}(\bar{x}_{rr}), \frac{\partial\bar{x}_z}{\partial t}, \ldots, \frac{\partial^{r-1}}{\partial t^{r-1}}(\bar{x}_z), \frac{\partial\bar{x}_{zz}}{\partial t}, \ldots, \frac{\partial^{r-1}}{\partial t^{r-1}}(\bar{x}_{zz}), \bar{u} \end{array}\right)\Bigg|_{r=0,z=L} \end{aligned} \tag{9}$$

The setpoint tracking calculator is applied to develop a correlation between $y - x_{p2}$. From the subsystem (7.a), the closed-loop response of the output at the center of the exit tube is in linear form as follows:

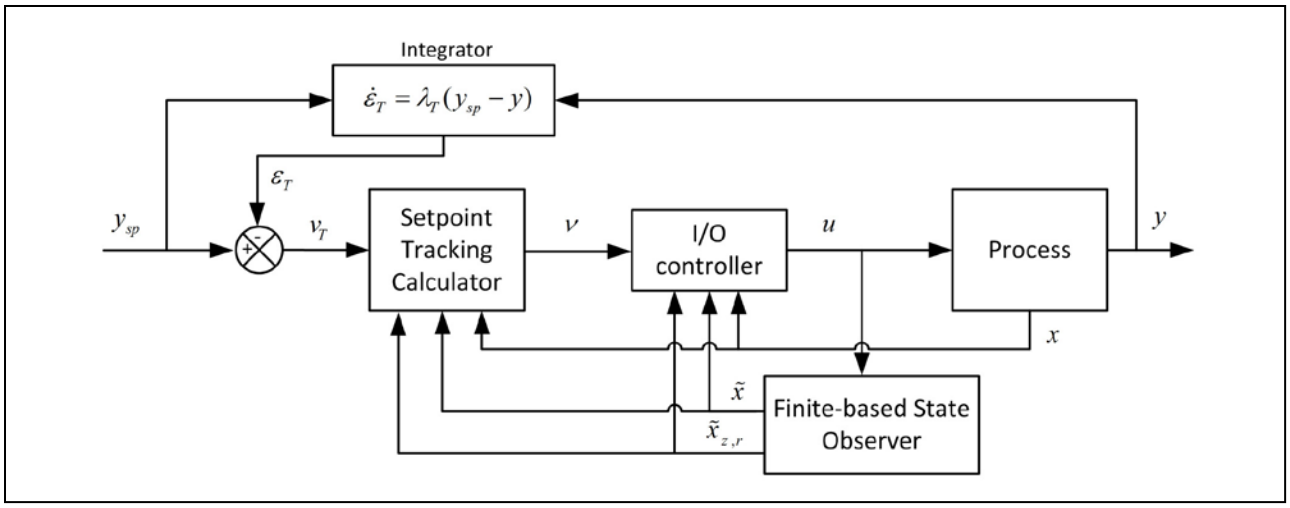

Fig. 2. Schematic diagram of the proposed control system.

$$(\varepsilon \mathcal{D}+1)^{r_1} y_L = y_{L,sp} \tag{10}$$

where $\mathcal{D}$ is the differential operator, y_L is the output at the position r=0 and z=L, $y_{L,sp}$ is the desired setpoint, ε is the tuning parameter used to adjust the speed of the output response and r_1 is the relative order of y_L with respect to x_{p2}.

By substituting the time derivatives of (9) into (10) and setting all time derivatives of the state gradients to be zero, the closed-loop responses of the output can be presented in a compact form

$$\phi_T(x_{p1}, x_{p1,r}, x_{p1,rr}, x_{p1,z}, x_{p2}) = y_{L,sp} \tag{11}$$

the tracking setpoint function (ν) of can be obtained by solving (11) for x_{p2}, in following form:

$$\nu = \psi_T(x_{p1}, x_{p1,r}, x_{p1,rr}, x_{p1,z}, x_{p2}, y_{L,sp}) \tag{12}$$

B. Feedback I/O linearizing controller

From the subsystem (7.b), the closed-loop responses of the state x_{p2} at the position z=L are requested in linear form as follows:

$$(\beta \mathcal{D}+1)^{r_2} x_{p2} = \nu \tag{13}$$

where ν is the tracking setpoint function, β is the tuning parameter and r_2 is the relative order of x_{p2} with respect to u.

We substitute the time derivative in (9) into (13) and set all time derivatives of the state gradients to be zero. The closed-loop responses of the state x_{p2} can be presented in a compact form

$$\phi_T(x_{p1}, x_{p2}, x_{zz}, u) = \nu \tag{14}$$

Thus, the feedback controller (u) is obtained by solving (14). The compact form of the controller equation is denoted by (15)

$$u = \Psi(x_{p1}, x_{p2}, x_{zz}, \nu) \tag{15}$$

C. Finite-based state observer

The CFD technique is a useful tool to predict behavior of the system of the complex PDE problem by using the numerical calculation. Thus, in this work, a CFD-based, open-loop state observer is developed to provide the estimation of the unmeasured process concentration, $\tilde{C}$, and the state derivatives.

D. Integrator

To compensate the process-model mismatch and the error from the estimate states, the first-order error dynamics in (16) is applied:

$$\begin{aligned} \dot{\varepsilon}_T &= \lambda_T (y_{sp} - y)\big|_{r=0, z=L} \\ \nu_T &= y_{sp} - \varepsilon_T \end{aligned} \tag{16}$$

where ε_T is the output error, λ_T is a positive parameter, and ν_T is the corrected setpoint.

IV. Result and Discussion

The velocity with plug-flow pattern is primarily assumed in many literatures for a control of the tubular reactor. However, this assumption is proper for a high viscosity fluid. To achieve a realistic prediction, the $k-\varepsilon$ turbulence model is applied with the developed 2D model, which the compared velocity profiles are shown in Fig.3.

For the servo test, the gas temperature at exit tube is controlled at the desired setpoint y_{sp}= 700 K. The initial conditions of the dynamics are C_{EDC}(r,0,t) = 359.83 mol/l, T_g (r,0,t)=644 K, T_t(0,t)= 716 K, and T_w=808 K. The tuning parameters of the proposed control system are ε=8, β=8 and λ=0.001. The closed-loop responses of the cracking furnace are illustrated in Figs. 4-6. The results show that

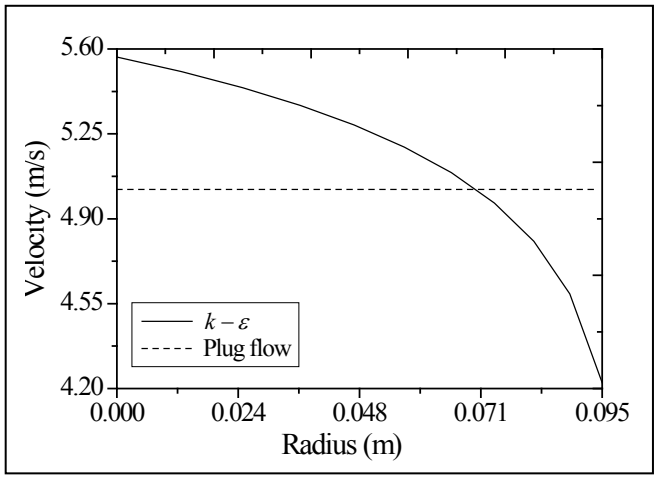

Fig.3. The flow pattern of cracked gas inside the tube.

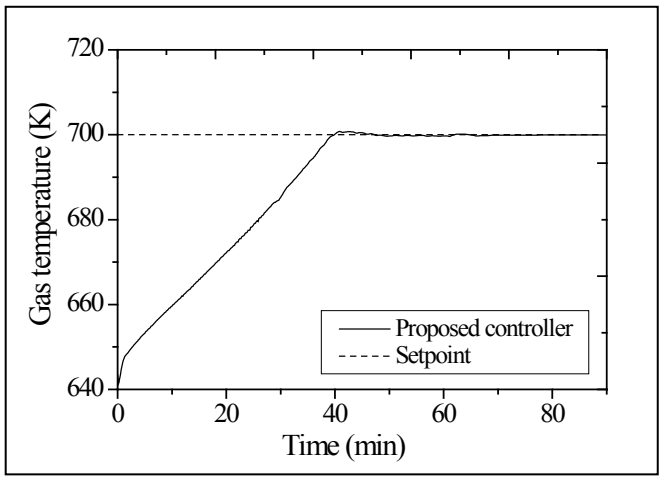

Fig.4. The closed-loop response of the gas temperature at the center exit tube.

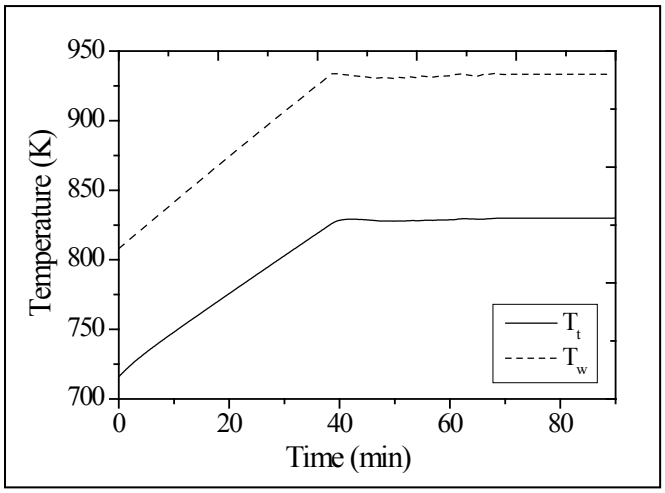

Fig.5. The closed-loop responses of the tube temperature at the exit and wall temperature.

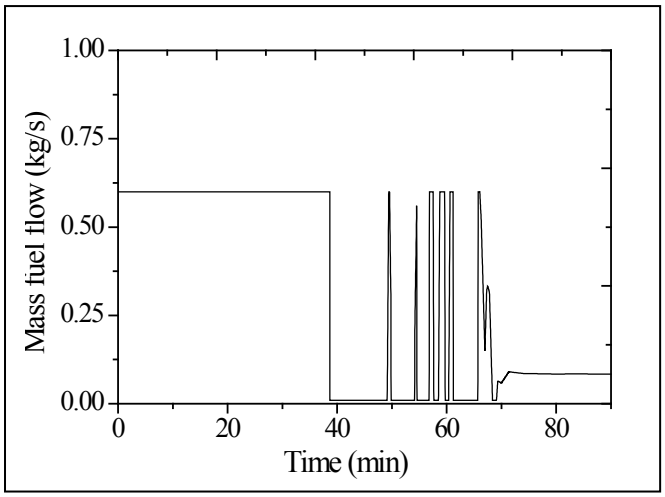

Fig.6. The control action of the manipulated input.

the controller successfully forces the gas temperature at the desired setpoint. The changes of gas, tube and wall temperature at the initial period have a linear trend due to the influence from the constant of fuel gas rate at the upper limit. The controller is then adjusted the fuel gas flow with a little fuzzy to put the gas temperature at the desired setpoint.

V. Conclusion

A new controller structure with I/O linearization technique is developed for the EDC cracking furnace, of which the advantages are a few tuning parameters and decrease on the complexity of the controller equation. With the importance of the distribution in r-direction of fluid flow in the tube, the $k-\varepsilon$ turbulent model is applied to the velocity. The controller is formulated with the 2D-PDEs and ODE into the setpoint tracking calculator and I/O feedback controller, and integrated with the first-order error dynamics and finite-based, open-loop observer. The simulation results show that the controller can force the control output at the desired setpoint effectively.

Acknowledgment

This work was financially supported by the Kasetsart University Research and Development Institute (KURDI), the project for Higher Education Research Promotion and National Research University Development, Office of the Higher Education Commission, and the Center of Excellence on Petrochemicals and Materials Technology. These supports are gratefully acknowledged.

References

[1] Shang, H., Fraser Forbes, J., Guay, M., 2005. Feedback control of hyperbolic distributed parameter systems. Chemical Engineering Science 60, 969–980.

[2] Hoo, K.A., Zheng, D., 2001. Low-order control-relevant models for a class of distributed parameter systems. Chemical Engineering Science 56, 6683–6710.

[3] Moghadam, A.A., Aksikas, I., Dubljevic, S., Forbes, J.F., 2010. LQ control of coupled hyperbolic PDEs and ODEs: Application to a CSTR–PFR system, in Proceedings of the Ninth International Symposium on Dynamics and Control of Process Systems. pp. 713–718.

[4] Yamuna Rani, K., Patwardhan, S.C., 2007. Data-Driven Model Based Control of a Multi-Product Semi-Batch Polymerization Reactor. Chemical Engineering Research and Design 85, 1397–1406.

[5] Aggelogiannaki, E., Sarimveis, H., 2009. Robust nonlinear H∞ control of hyperbolic distributed parameter systems. Control Engineering Practice 17, 723–732.

[6] Masoumi, M.E., Sadrameli, S.M., Towfighi, J., Niaei, A., 2006. Simulation, optimization and control of a thermal cracking furnace. Energy 31, 516–527.

[7] Zeybek, Z., 2006. Role of adaptive heuristic criticism in cascade temperature control of an industrial tubular furnace. Applied Thermal Engineering 26, 152–160.

[8] Panjapornpon, C., Limpanachaipornkul, P., Charinpanitkul, T., 2012. Control of coupled PDEs–ODEs using input–output linearization: Application to a cracking furnace. Chemical Engineering Science 75, 144–151.

[9] Van Geem, K.M., Heynderickx, G.J., Marin, G.B., 2004. Effect of radial temperature profiles on yields in steam cracking. AIChE journal 50, 173–183.

[10] Han, Y.L., Xiao, R., Zhang, M.Y., 2007. Combustion and Pyrolysis Reactions in a Naphtha Cracking Furnace. Chemical Engineering & Technology 30, 112–120. doi:10.1002/ceat.200600191.

[11] Mercado, E.R.L., Nunhez, J.R., 2000. Modelagem do aquecimento de fluidos com escoamento em tubos [WWW Document]. URL http://www.bibliotecadigital.unicamp.br/document/?code=vtls000197788 (accessed 1.20.14).

[12] Incropera, F., Dewitt, D., 2002. Fundamentals of Heat and Mass Transfer, 5th ed. John Wiley & Sons, New York